Published in final edited form as:
J Chem Inf Model. 2011 September 26; 51(9): 2417–2426. doi:10.1021/ci200280m.

Discovery of Novel Selective Serotonin Reuptake Inhibitors Through Development of a Protein-Based Pharmacophore

Sankar Manepalli[a], **Laura M. Geffert**[b], **Christopher K. Surratt**[b], and **Jeffry D. Madura**[a]

[a]Department of Chemistry and Biochemistry and Center for Computational Sciences, Duquesne University, 600 Forbes Avenue, 308 Mellon Hall, Pittsburgh, PA 15282, USA

[b]Division of Pharmaceutical Sciences, Mylan School of Pharmacy, Duquesne University, 600 Forbes Avenue, 411 Mellon Hall, Pittsburgh, PA 15282, USA

Abstract

The serotonin transporter (SERT), a member of the neurotransmitter sodium symporter (NSS) family, is responsible for the reuptake of serotonin from the synaptic cleft to maintain neurotransmitter homeostasis. SERT is established as an important target in the treatment of anxiety and depression. Because a high-resolution crystal structure is not available, a computational model of SERT was built based upon the x-ray coordinates of the leucine transporter LeuT, a bacterial NSS homolog. The model was used to develop the first SERT structure-based pharmacophore. Virtual screening (VS) of a small molecule structural library using the generated SERT computational model yielded candidate ligands of diverse scaffolds. Pharmacological analysis of the VS hits identified two SERT-selective compounds, potential lead compounds for further SERT-related medication development.

Introduction

Signaling between cells in the central nervous system is mediated by the controlled release and reuptake of neurotransmitters in the synapse.[1] An excess or deficit of the monoamines serotonin, dopamine or norepinephrine in the synapse has been associated with various psychiatric and neurological disorders including depression, anxiety, compulsivity, attention deficit hyperactivity disorder (ADHD), substance abuse, Parkinson's disease and schizophrenia. [2–7] Control of synaptic monoamine levels is affected by the plasma membrane monoamine transporters (MATs), which terminate the action of these biogenic amines via reuptake into the presynaptic cell. The mechanisms of action of drugs related to the above medical conditions typically involve the MAT proteins. Tricyclic antidepressants (TCAs) such as imipramine (Tofranil™), developed in the 1950s, alleviate depression by blocking serotonin and norepinephrine transporters (SERT and NET, respectively), thereby extending the lifespan of synaptic serotonin and norepinephrine. Unfortunately, the TCAs also block adrenergic, muscarinic acetylcholine and histamine receptors, responsible for a plethora of adverse effects.[8, 9] Selective serotonin reuptake inhibitors (SSRIs), the next generation of antidepressants led by fluoxetine (Prozac™) in the 1980s, carry far fewer adverse effects compared to the TCAs. The SSRIs block SERT, but because the resultant surge of serotonin can activate any of 14 serotonin receptor types, this drug class is not without its own adverse effects.[10–12]

The driving force for MAT uptake of monoamine substrate is electrogenic, harnessing the inward Na^+ gradient across the cell membrane.[13, 14] The SERT, NET and DAT (dopamine

Correspondence to: Jeffry D. Madura.

transporter) are members of the neurotransmitter:sodium symporter (NSS) family as well as members of a larger group of Na^+ and Cl^- dependent transporters known as the "solute carrier 6" (SLC6) family.[15] The lack of a high-resolution 3-D MAT structure had hindered structure-function and therapeutic development efforts until a breakthrough was achieved in the form of crystallization of the bacterial NSS homolog LeuT, a leucine transporter.[16] The LeuT x-ray structure has provided a template to build credible MAT computational models.[16–21] Although model quality increases with sequence identity with the template, structural similarity also plays a significant role.

In the absence of high-resolution 3D structures for SERT, development of a ligand based pharmacophore[22–25] or QSAR[26–28] are feasible alternatives to obtain structural information about the binding pocket. Ligand-based approaches analyze a set of ligands and generate possible protein-ligand interaction patterns without knowledge of the protein structure. A limitation of ligand-based approaches is that flexible alignment using dissimilar scaffolds is less reliable; knowledge of the bioactive conformation of at least one active molecule significantly improves alignment accuracy.[29] These limitations can be overcome by using structure-based approaches, in which diverse scaffolds can be used to capture ligand interactions and the binding pocket environment in general. Docking, a structure-based technique, is capable of reliably predicting the bioactive conformation for a co-crystallized ligand.[30] In the absence of an experimental 3D structure, however, a reasonable 3D model can be constructed for a receptor using crystallographic or NMR data from genetically and functionally related proteins.[31, 32]

Comparative modeling correctly predicts the 3D fold of a protein in most cases and has often provided insight into the atomistic details of ligand binding.[33, 34] Models created by this method have identified potential binding pockets, and have been employed for docking, structure-based pharmacophore generation and virtual screening (VS) to identify new ligands and their interactions with the protein.[33, 35, 36] Pharmacophore models, defined as a 3D collection of features essential for bioactivity of a ligand, have been widely employed.[37, 38] The approach of combining a pharmacophore with VS has yielded novel structural scaffolds for ligands of a target receptor.[39–44] Application of this technique with the DAT led to the identification of structurally novel VS "hit" compounds which, upon further modification, created a more potent analog through rational drug design.[33, 43, 45] The present work describes the development of a structure-based pharmacophore and its VS utilization to identify novel ligand structural scaffolds that display SERT selectivity.

Results and Discussion

Four discrete amino acid sequence alignments with LeuT were generated that primarily differed in the loop regions. Manual refinement of the alignments was conducted to remove gaps within the TM regions. Rotamers of the residue side chains lining the hSERT halogen-binding pocket were selected based on their ability to form a sub-pocket, as these residues have been reported to be important for binding of certain SSRIs.[21] A total of 80 SERT homology models were built using Discovery Studio (DS) 2.5.1. Five models from each alignment (20 models total) having the lowest discrete optimized protein energy (DOPE) score were chosen for further evaluation. DOPE is an atomistic-based statistical potential for model evaluation and structure prediction. This conformational energy measure reflects the stability of a model relative to other models generated. [46] The models were also deposited into the PDB evaluation server and assessed with respect to stereochemical quality.[47 (accessed Sep 30, 2010)] The plots generated by the server were evaluated for unusual phi-psi angles, bond lengths, bond angles and van der Waals contacts. Two models were selected for further evaluation, specifically their fitness in a 3D environment assessed by Profiles-3D. This DS module assesses the protein's tertiary structure compatibility with its

sequence. Finally, spatial overlap of the model and template polypeptide backbone atoms was examined to check the integrity of the model's TM domains and the volume of its binding pocket. On this basis, "Model 1" was chosen for further studies.

The MOE alpha site finder was used to identify possible ligand sites in Model 1. A site exposed to the extracellular space was chosen based on evidence for inhibitors binding in this vestibule.[21] A sphere with a radius of 8 Å was created to constrain the resulting docked poses, in keeping with recent reports.[18, 21] The combination of proxy triangle as the placement method and force field refinement with an affinity scoring function yielded MOE docking poses of leucine into LeuT with an RMSD of 0.31 Å (data not shown). This strategy was next used to dock each of 16 structurally diverse antidepressants (Figure 1), possessing a large range of SERT binding affinities (0.1 nM – 9100 nM). It is acknowledged that certain SSRI ligands used in the docking have been reported to access the interior S1 substrate pocket [48]; however, the VS pocket employed in this study contained elements of the vestibular (S2 substrate) pocket and the halogen binding pocket (HBP) (Figure 2A). The latter pocket is defined in part by hSERT residues Leu-99 (TM 1), Trp-103 (TM 1) and Ile-179 (TM 3). The ligand-accessible region of the HBP (green cloud) is adjacent to that of the S2 pocket (orange cloud) (Figure 2A); the HBP appears to be important for recognition of halogen-containing inhibitors. Poses in which the halogen atom of the ligand was directed toward this pocket were thus favored. A consensus was developed by overlaying the highest-ranked poses to generate a "common interaction pattern".

Residues identified as common interaction points were then chosen to develop a 3D pharmacophore (Figure 2B). Pharmacophore feature F1 of radius 1 Å was created midway between Arg-104 (TM 1) and Glu-493 (TM 10) to capture possible ionic or H-bond interactions, particularly with protonated ligand nitrogen atoms. Previous reports of SERT-based pharmacophore models indicated the importance of a positively charged nitrogen atom.[49, 50] Feature F2 (radius 1 Å) was created in the vicinity of Lys-490 (TM 10) to capture possible H-bond interactions. The lysine side chain is among the more flexible of the naturally occurring amino acids; 78 rotamers were possible for Lys-490. The rotamer oriented toward the vestibular pocket, analogous to Asp-401 in LeuT, was chosen to capture possible interactions with ligands. Asp-401 is reported to interact with different antidepressants in LeuT crystal structures[21]; thus, Lys-490 would be expected to play a similar role in hSERT. Feature F3 (radius 1 Å) was created to capture H-bond or cation-π interactions with Tyr-107 (TM 1). Residues 104–106 of hSERT TM 1b are analogous to LeuT residues 30–32, although hSERT Tyr-107 and LeuT Val-33 differ substantially regarding the nature of potential ligand interactions. Feature F4 (radius 1.5 Å) in the HBP was designed for hydrophobic interactions believed to be important in recognizing SSRIs. Residues lining the pocket are conserved between hSERT and LeuT.[21] Substitution of the hSERT TM 3 residue Ile-179 (Ile-111 in LeuT) with alanine, phenylalanine or aspartic acid increased SSRI substrate uptake inhibition potency by 7 – 1080 fold.[21] The TM 1 mutations Ala77Gly in hNET and Ala81Gly in hDAT were observed to improve SSRI affinity, suggesting a negative influence of the methyl side chain of alanine on SSRI binding. Finally, an exclusion volume was added to make the pharmacophore more stringent and selective.

Approximately one million members of the ZINC small molecule structural library database[51] were screened with the hSERT pharmacophore for possible "hit" compounds (those predicted to be SERT ligands). A total of 4097 molecules were acceptable to the pharmacophore filter. Docking of this subset into the SERT model followed by monitoring of affinity dG scores with visual inspection of the resulting poses yielded 68 preferred compounds. Due to lack of availability, only ten of the top 15 compounds (labelled SM-1 to SM-15) were initially tested for hSERT, hDAT or hNET affinity in single point in vitro binding assays. Two compounds, SM-10 and SM-11, at 10 μM significantly displaced the

cocaine analog [^{125}I]-RTI-55 from hSERT membranes, indicating measurable hSERT affinity. At the same final concentration, these two compounds did not displace the radioligand at hDAT or hNET cells. SM-14, curiously, displaced [^{125}I]-RTI-55 at hDAT cells alone (Figure 3). A DAT binding affinity K_i value of 15.6 ± 2.4 μM (mean ± s.e.m.) and a dopamine uptake inhibition potency IC_{50} value of 10.5 ± 4.6 μM were observed (manuscript in preparation). SM-10 and SM-11 were further characterized at hSERT HEK293 membranes in competition assays to obtain K_i values for inhibition of [^{125}I]-RTI-55 binding. hSERT K_i values of 38 ± 17 μM and 17 ± 7 μM were obtained for SM-10 and SM-11, respectively (Figure 4). SM-10 and SM-11 were also screened for the ability to inhibit uptake of [^{3}H]-serotonin by intact hSERT HEK293 cells. Because no inhibition of [^{3}H]-serotonin uptake was detected at the 10 μM final concentration employed for these two VS hit compounds (Figure 5), IC_{50} values were not obtained. Given their structural flexibility (Figure 6), SM-10 and SM-11 greatly differ from the SSRIs and TCAs that were employed to develop the pharmacophore.

Given the high sequence similarity (~ 50%, as calculated with BLAST) among the three-hMATs, finding a specific inhibitor that targets a single transporter is a challenging task. VS is more precarious with the additional inhibitor binding pocket uncertainty associated with a homology model built using a template sharing < 30% sequence identity (Figure 7). Because of this handicap, and because the goal of the study was to identify SERT ligands of novel structural scaffold, a very high concentration of VS hit compound relative to the SERT ligand radiotracer (100,000-fold) was employed in the pharmacologic screen. The observation that most of the VS hits showed no ability to displace the radioligand at the SERT-HEK cells confirms that the huge molar ratio of VS compound:radiotracer was itself insufficient for decreasing radiotracer binding (*i.e.*, some SERT affinity is required to register a response in this assay).

The two VS hits pharmacologically verified as SERT ligands displayed micromolar K_i values. These binding affinities are very low compared to the nanomolar or better SERT affinities of certain SSRI therapeutics. Inhibition of serotonin uptake was not observed for any VS hit compound at the 10 μM screening concentration. Substrate uptake inhibition potency is often lower than binding affinity for a given MAT inhibitor, possibly due to differences in MAT conformational or population requirements for the two processes.[52, 53] The 10 μM SM-10 or SM-11 concentration employed may be above the threshold for detecting SERT ligand binding but below the threshold for detecting serotonin uptake inhibition.

Micromolar affinities for VS hit compounds are common when homology models are employed.[54–61] From this research team, the first reported VS effort based on a DAT homology model yielded a hit compound (MI-4) with low micromolar DAT affinity and slightly better (high nanomolar) SERT affinity. Without modification, this compound displayed antipsychostimulant and antidepressant properties (Ref. 43 and unpublished data). The same VS effort using a DAT model yielded a hit compound (MI-17) with a SERT K_i value of 284 nM. An MI-17 analog designed to increase SERT selectivity resulted in a compound with a SERT K_i value of 37 nM, and SERT:DAT and SERT:NET selectivity ratios of 50 and over 200, respectively.[45] Thus, VS hit compounds with micromolar affinities appear to be useful as lead compounds for medication development.

Conclusion

To our knowledge this is the first study to identify novel SERT-selective reuptake inhibitors through VS performed with an hSERT homology model. Conventional drug development usually involves creation of analogs of established ligands for a given receptor. In contrast,

the VS approach affords the possibility of discovering ligands with very different scaffolds, ligands that in all likelihood would never be otherwise identified for that receptor. In the case of the SERT, inhibitors of novel scaffold provide new opportunities for development of rationally designed multi-site drugs (*e.g.*, SERT/5-HT_{2A}/5-HT_3 blockers) that address the therapeutic goal while mitigating the adverse effects associated with the SSRI drug class. It is anticipated that the two SM compounds described herein should serve as lead compounds toward the treatment of depression, anxiety, and other serotonin-related disorders.

Methods

Materials

[^{125}I]-RTI-55 and [^{3}H]-serotonin were purchased from PerkinElmer (Foster City, CA). VS hit compounds were purchased from enamine and molport. The N2A-hDAT cell line was a gift from Dr. Margaret Gnegy (University of Michigan). HEK293 cells stably transfected with hSERT or hNET were prepared in collaboration with Dr. Mads Larsen and Dr. Susan Amara (University of Pittsburgh, Pittsburgh, PA).

Construction of SERT homology models

Polypeptide sequence retrieval and alignment—The FASTA sequence for human SERT was downloaded from the Uniprot database (accession number P31645).[62] The x-ray crystal structure of the *Aquifex aeolicus* protein LeuT (2a65) was used as a template and downloaded from the Protein Data Bank (PDB).[63] The template was checked for missing residues using the "protein reports and utilities" module in Discovery Studio (DS) 2.5.1.[64] Prior to modeling efforts, the missing residues Asn-133 and Ala-134 of the second extracellular loop (EL2) were built into the LeuT template and subjected to the DS loop refinement protocol. Different hSERT models were created using the Align2d methodology[65] and the three previously proposed sequence alignments. [16, 66, 67]

hSERT Model 1: Manepalli et al. alignment (this article)—The sequences of hSERT and modified LeuT were aligned using the "align sequence to templates" protocol in DS. An alignment similar to Celik et al.[66] was generated, with minor manual modifications further increasing the sequence identity with LeuT (Figure 7). N- and C-terminal overhangs were deleted, increasing sequence identity to 24% and sequence similarity to 47%. The hSERT model sequence began at Arg-79 in the N-terminal tail and ended with Lys-605 in the C-terminal tail. The "build homology model" protocol in DS, which employs MODELLER version 9v4,[31] was used to construct 20 hSERT models. The models were further refined (see "Model validation") and ranked by discrete optimized protein energy[46] (DOPE) score. The model with the best DOPE score was designated "Model 1".

hSERT Model 2: Beuming et al. alignment—The hSERT query sequence and modified LeuT were loaded into DS and aligned as described by Beuming et al.[67] Terminal residues not having the matching template coordinates at both ends were omitted, and 20 models were built and assigned DOPE scores as described above. Models based on this alignment resulted in EL2 positioned directly above the substrate permeation pore, which would likely have influenced ligand docking. The dangling EL2 was adjusted using the DS loop refinement protocol. Models were then evaluated using the "verify protein" protocol, which assesses the score of each residue in the known 3D environment. This was followed by superposition of the hSERT model onto LeuT to check for TM domain coincidence. The final version was designated "Model 2".

hSERT Model 3: Yamashita et al. alignment—The hSERT query sequence and modified template were aligned as proposed by Yamashita et al.[16] N- and C-terminal

overhangs were deleted, leaving 527 hSERT residues. The optimal model resulting from this alignment was designated as “Model 3”.

hSERT Model 4: Celik et al. alignment—Twenty hSERT models were built with DS as described above but following the proposed Celik et al. alignment[66], which offered a sequence identity match comparable to the Manepalli alignment and greater than the Beuming and Yamashita alignments. A 527-residue hSERT polypeptide was used to develop “Model 4”, as described for Model 1.

Model Refinement and Validation

Five models from each of the four alignment groups were chosen based on DOPE scores. The stereochemical quality of the preferred models was assessed with the validation server used to evaluate structures deposited into PDB.[46] From each group of five, two models were then chosen based on their having the fewest outliers on the phi-psi angle Ramachandran plot. These two models were evaluated for 3D fold, using the “verify protein” protocol in DS. This protocol reduces 3D structures to a simplified 1D representation, compares this to the 1D amino acid sequence, and assigns a score. This score is compared to the expected high and low scores for the sequence predicted from statistical analysis of high-resolution PDB structures.

TM domain assembly and ligand binding pocket volume were checked by superposing the SERT models onto the LeuT model using MOE (Figure 8).[68] A single hSERT model was selected for each of the four groups. The all-atom force field AMBER99 [69, 70] was used to add hydrogen atoms and partial charges to the models. Keeping the non-hydrogen atoms fixed in space, hydrogen atoms were minimized with a convergence criterion of 0.05 kcal/mol. The final hSERT models chosen from each alignment were further optimized to minimize the outliers and avoid unnecessary protein contacts. Of the four models, Model 1 had the smallest RMSD on superposition with LeuT and maximal ligand binding pocket volume, similar to the LeuT.

Ligand binding site delineation and docking; pharmacophore development

The alpha site finder function of MOE 2008.09 was used to identify possible ligand binding sites in Model 1. The site finder is purely geometric; no energy terms are used. Alpha spheres within the hSERT model that were too exposed to solvent were eliminated; spheres that corresponded to locations of tight atomic packing in the model were retained. Spheres were classified as either “hydrophobic” or “hydrophilic” depending on the potential for hydrogen bonding. Following the default settings, alpha spheres were clustered to produce a collection of putative binding sites that are ranked according to the number of hydrophobic atoms within contact distance of the spheres. Finally, dummy atoms were created in the S1 and S2 pockets to specify the algorithm to dock the ligands.

Ligand coordinates were obtained from the small molecule crystal database CCSD (Cambridge Crystallographic Structural Database).[71, 72] Ligands having no coordinates were drawn using MOE. Partial charges and hydrogen atoms were added to all ligands using Merck Molecular Force Field 94X (MMFF94x).[73–75] Ligand geometry was optimized via energy minimization with a conjugated gradient truncated Newton optimization algorithm with convergence criteria = 0.01 kcal/mol, ε = 1. Leucine or selected TCA drugs were first docked with the LeuT model to test for consistency with the reported cocrystal structures.[16, 21] Atom placement methods including proxy triangle, alpha triangle and triangle matcher were employed, as were refinement techniques using grid-based and force field-based methods. The combination that produced poses very close to the crystal structure (<1Å) was chosen for hSERT docking. Interaction plots for all docked poses of different

antidepressants in hSERT were generated using the MOE ligand interaction module.[76] A consensus of residues and their predicted ligand interactions was developed and used in creating the pharmacophore features for the vestibular ligand-binding pocket.

A pharmacophore feature was generated at each amino acid side chain – ligand interaction point obtained from initial docking iterations. Pharmacophore points F1, F2, F3 (each with a radius of 1 Å) and F4 (radius = 1.5 Å) were delineated to better encompass the hydrophobic features of the docked ligands. An excluded volume was created, and the algorithm assigned a penalty to poses that encroached on this space. The final pharmacophore product was tested using a database containing known hSERT ligands and decoy ligands. The pharmacophore model successfully discriminated the classic hSERT ligands from the decoys.

Virtual Screening

An 18 million entry "all-purchasable" subset of the ZINC database containing was downloaded.[51] The subset was "washed" by importing the collection into MOE, which removes unwanted salts, ions and disconnected molecular fragments from the database. The Lipinski's Rule of Five descriptor was applied to the database to remove nondrug-like molecules.[77] Compounds with reactive groups were removed by further screening the database using a toxic moiety descriptor. From this database a subset containing approximately one million compounds was selected for further use. Tautomers and protomers of these entries were generated at physiological pH. Using the "import conformation" module of MOE, different conformations were generated and minimized using the MMFF94x force field; conformations with strain energy 4 kcal/mol or more above the lowest energy conformation were discarded. This final database was screened using the 4-point pharmacophore. "Hit" compounds acceptable to the pharmacophore filter were further screened to ensure the presence of halogens and a molecular weight < 350 daltons, features common to most of the known antidepressants. These steps yielded a pool of 4,097 hit compounds. Three hSERT docking iterations were performed with this pool of structures. Affinity scores < −6.0 kcal/mol plus visual inspection was used to condense the pool to 68 candidate ligands. Of these, 10 of the top-ranked 15 compounds (coded "SM-1" through "SM-15") were procured from various sources and pharmacologically tested.

Pharmacology

In vitro VS compound binding screen—Compounds identified from the virtual screen were purchased and dissolved in 100% DMSO to a concentration of 10 mM. Initial one-point competition binding assays were conducted using 10 μM final concentration of VS hit compound and 0.1 nM of the radiolabeled cocaine analog [^{125}I]-RTI-55, a radioligand with high affinity at all three MATs. Stably transfected HEK293-hSERT membranes or N2A-hDAT or HEK293-hNET whole cells were employed for all binding assays. Non-specific binding was determined by inclusion of 10 μM paroxetine, mazindol or desipramine for hSERT, hDAT or hNET assays, respectively. Screening results were analyzed with one-way ANOVA ($P < 0.05$) with a post-hoc Dunnett's Multiple Comparison Test.

hSERT membrane binding assay—hSERT binding affinities were obtained by displacement of [^{125}I]-RTI-55 in membrane binding assays. Membrane was prepared from stable hSERT-HEK cells grown at 37°C in a 5% CO_2 environment on 150 × 25 mm plates. At 95% confluence (3 days of growth), cells were washed twice with 10 mL cold phosphate-buffered saline (DPBS). An additional 10 mL of DPBS was added and cells were harvested by scraping and transferred to cold centrifuge tubes (15 mL), followed by centrifuging for 10 min at low speed (700 × g). After removal of the supernatant, the cell pellet was resuspended in 500 uL cold TE buffer (50 mM Tris, 1 mM EDTA, pH 7.5). Following

centrifuging for 30 min at 100,000 × g at 4°C, the supernatant was discarded and the pellet was frozen for later use or resuspended in ice-cold binding buffer (50 mM Tris, pH 7.5, 100 mM NaCl). Each sample was analyzed for protein content using the Bradford protein assay. For competition binding, membrane was incubated with [^{125}I]-RTI-55 (0.1 nM concentration) and increasing concentrations of cold competitor (1 nM to 1 mM), or 10 μM paroxetine to measure non-specific binding. Reactions were carried out in 12 × 75 mm borosilicate glass tubes with gentle shaking at room temperature for 1 hour and terminated by rapid filtration through GF/B filters (Schleicher and Schuell, Keene, NH) presoaked in 0.5% polyethylenimine solution (v/v). Filters were washed twice with 5 mL cold 50 mM Tris buffer and transferred to vials. Radioactivity was determined using a Beckman gamma counter. For saturation binding assays, data were analyzed with GraphPad Prism 5.0 software. IC_{50} values were generated and converted to K_i values using the Cheng-Prusoff equation ($K_i = IC_{50}/(1+ ([RTI-55]/K_d$ RTI-55)).[78]

hDAT and hNET whole cell binding assays—Whole-cell competition binding assays were performed for hDAT and hNET using stable hDAT-N2A or hNET-HEK293 cell lines, respectively, grown at 37°C in a 5% CO_2 environment. Cell monolayers were grown in 24-well plates to >90% confluence. Cells were washed twice with 1 mL of KRH buffer (25 mM HEPES, pH 7.3, 125 mM NaCl, 4.8 mM KCl, 1.3 mM $CaCl_2$, 1.2 mM $MgSO_4$, 1.2 mM KH_2PO_4, 5.6 mM glucose) supplemented with 50 mM ascorbic acid (KRH/AA). Cells were incubated for 15 minutes with 1 nM [^{125}I]-RTI-55 supplemented with tropolone (total volume of 500 uL) along with increasing concentrations of drug or 10 μM mazindol (hDAT) or 10 μM desipramine (hNET). Following incubation, cells were washed twice with 1 mL KRH/AA buffer, then treated with 1 mL 1% SDS with gentle shaking at room temperature for 1 hour. Cell lysates were transferred into vials. Radioactivity was determined using a Beckman gamma counter and analyzed using GraphPad Prism 5.0 as described above.

Serotonin uptake inhibition screen—One-point competition binding assays were performed using stably transfected HEK293-hSERT whole cells grown to >90% confluence on 24-well plates. Cells were washed with KRH buffer, then preincubated with 10 μM VS hit compound for 10 min, followed by addition of 10 nM [^{3}H]-serotonin. After an additional 5 min, cells were washed twice, then treated with 1% SDS and shaken for 1 hr. Lysates were transferred to 5 mL scintillation fluid and radioactivity was detected using a Beckman liquid scintillation counter. Non-specific radioligand uptake was determined in the presence of 10 μM clomipramine.

Acknowledgments

We thank Dr. Tammy Nolan for creating the hSERT and hNET HEK cell lines and for helpful discussions in the development of the manuscript, and thank Drs. Mads Larsen and Susan Amara for collaboration in creating the hSERT and hNET cell lines. This work was supported by NIDA grants DA026350 (to C.K.S) and NIH grant DA027806, Department of Education equipment grants P116Z050331 and P116Z080180 (to J.D.M).

Abbreviations

MAT	monoamine transporter protein
hSERT	plasma membrane human serotonin transporter protein
hDAT	plasma membrane human dopamine transporter protein
hNET	plasma membrane human norepinephrine transporter protein
SSRI	selective serotonin reuptake inhibitor

VS	virtual screening
DOPE	discrete optimized protein energy

References

1. Amara SG, Kuhar MJ. Neurotransmitter transporters: Recent progress. Annu Rev Neurosci. 1993; 16:73–93. [PubMed: 8096377]
2. Hahn MK, Blakely RD. Monoamine transporter gene structure and polymorphisms in relation to psychiatric and other complex disorders. Pharmacogenomics J. 2002; 2(4):217–235. [PubMed: 12196911]
3. Heinz A, Mann K, Weinberger DR, Goldman D. Serotonergic dysfunction, negative mood states, and response to alcohol. Alcohol Clin Exp Res. 2001; 25(4):487–495. [PubMed: 11329486]
4. Klimek V, Stockmeier C, Overholser J, Meltzer HY, Kalka S, Dilley G, Ordway GA. Reduced levels of norepinephrine transporters in the locus coeruleus in major depression. J Neurosci. 1997; 17(21):8451–8458. [PubMed: 9334417]
5. Robertson D, Flattem N, Tellioglu T, Carson R, Garland E, Shannon JR, Jordan J, Jacob G, Blakely RD, Biaggioni I. Familial orthostatic tachycardia due to norepinephrine transporter deficiency. Ann N Y Acad Sci. 2001; 940:527–543. Neuro-Cardiovascular Regulation. [PubMed: 11458707]
6. Miller GM, De La Garza R II, Novak MA, Madras BK. Single nucleotide polymorphisms distinguish multiple dopamine transporter alleles in primates: Implications for association with attention deficit hyperactivity disorder and other neuropsychiatric disorders. Mol Psychiatry. 2001; 6(1):50–58. [PubMed: 11244485]
7. Ozaki N, Goldman D, Kaye WH, Plotnicov K, Greenberg BD, Lappalainen J, Rudnick G, Murphy DL. Serotonin transporter missense mutation associated with a complex neuropsychiatric phenotype. Mol Psychiatry. 2003; 8(11):933–936. [PubMed: 14593431]
8. Cusack B, Nelson A, Richelson E. Binding of antidepressants to human brain receptors: focus on newer generation compounds. Psychopharmacology. 1994; 114(4):559–565. [PubMed: 7855217]
9. Green JP, Maayani S. Tricyclic antidepressant drugs block histamine H2 receptor in brain. Nature. 1977; 269(5624):163–165. [PubMed: 20581]
10. Ferguson JM. SSRI Antidepressant Medications: Adverse Effects and Tolerability. Prim Care Companion J Clin Psychiatry. 2001; 3(1):22–27. [PubMed: 15014625]
11. Frazer A. Pharmacology of antidepressants. J Clin Psychopharmacol. 1997; 17 (Suppl 1):2S–18S. [PubMed: 9090573]
12. Goldberg RJ. Selective Serotonin Reuptake Inhibitors: Infrequent Medical Adverse Effects. Arch Fam Med. 1998; 7(1):78–84. [PubMed: 9443704]
13. Rudnick G. Mechanisms of biogenic amine neurotransmitter transporters in: Neurotransmitter transporters: structure, function, and regulation. 1997:73–100.
14. Masson J, Sagne C, Hamon M, El Mestikawy S. Neurotransmitter transporters in the central nervous system. Pharmacol Rev. 1999; 51(3):439–464. [PubMed: 10471414]
15. Nelson N. The family of Na+/Cl− neurotransmitter transporters. J Neurochem. 1998; 71(5):1785–1803. [PubMed: 9798903]
16. Yamashita A, Singh SK, Kawate T, Jin Y, Gouaux E. Crystal structure of a bacterial homologue of Na+/Cl−-dependent neurotransmitter transporters. Nature. 2005; 437(7056):215–223. [PubMed: 16041361]
17. Zhou Z, Zhen J, Karpowich NK, Goetz RM, Law CJ, Reith MEA, Wang D-N. LeuT-Desipramine Structure Reveals How Antidepressants Block Neurotransmitter Reuptake. Science. 2007; 317(5843):1390–1393. [PubMed: 17690258]
18. Singh SK, Yamashita A, Gouaux E. Antidepressant binding site in a bacterial homologue of neurotransmitter transporters. Nature. 2007; 448(7156):952–956. [PubMed: 17687333]
19. Singh SK, Piscitelli CL, Yamashita A, Gouaux E. A Competitive Inhibitor Traps LeuT in an Open-to-Out Conformation. Science. 2008; 322(5908):1655–1661. [PubMed: 19074341]

20. Quick M, Lund Winther A-M, Shi L, Nissen P, Weinstein H, Javitch JA. Binding of an octylglucoside detergent molecule in the second substrate (S2) site of LeuT establishes an inhibitor-bound conformation. Proc Natl Acad Sci. 2009; 106(14):5563–5568. [PubMed: 19307590]
21. Zhou Z, Zhen J, Karpowich NK, Law CJ, Reith ME, Wang DN. Antidepressant specificity of serotonin transporter suggested by three LeuT-SSRI structures. Nat Struct Mol Biol. 2009; 16(6): 652–657. [PubMed: 19430461]
22. Orus L, Perez-Silanes S, Oficialdegui A-M, Martinez-Esparza J, Del Castillo J-C, Mourelle M, Langer T, Guccione S, Donzella G, Krovat EM, Poptodorov K, Lasheras B, Ballaz S, Hervias I, Tordera R, Del Rio J, Monge A. Synthesis and Molecular Modeling of New 1-Aryl-3-[4-arylpiperazin-1-yl]-1-propane Derivatives with High Affinity at the Serotonin Transporter and at 5-HT1A Receptors. J Med Chem. 2002; 45(19):4128–4139. [PubMed: 12213056]
23. Zhang S, Fernandez F, Hazeldine S, Deschamps J, Zhen J, Reith MEA, Dutta AK. Further Structural Exploration of Trisubstituted Asymmetric Pyran Derivatives (2S,4R,5R)-2-Benzhydryl-5-benzylamino-tetrahydropyran-4-ol and Their Corresponding Disubstituted (3S,6S) Pyran Derivatives: A Proposed Pharmacophore Model for High-Affinity Interaction with the Dopamine, Serotonin, and Norepinephrine Transporters. J Med Chem. 2006; 49(14):4239–4247. [PubMed: 16821783]
24. Chang C, Ekins S, Bahadduri P, Swaan PW. Pharmacophore-based discovery of ligands for drug transporters. Adv Drug Delivery Rev. 2006; 58(12–13):1431–1450.
25. MacDougall IJA, Griffith R. Pharmacophore design and database searching for selective monoamine neurotransmitter transporter ligands. J Mol Graphics Modell. 2008; 26(7):1113–1124.
26. Wellsow J, Machulla H-J, Kovar K-A. 3D QSAR of serotonin transporter ligands: CoMFA and CoMSIA studies. Quant Struct-Act Relat. 2002; 21(6):577–589.
27. Pratuangdejkul J, Schneider B, Jaudon P, Rosilio V, Baudoin E, Loric S, Conti M, Launay JM, Manivet P. Definition of an uptake pharmacophore of the serotonin transporter through 3D-QSAR analysis. Curr Med Chem. 2005; 12(20):2393–2410. [PubMed: 16181139]
28. Kharkar Prashant S, Reith Maarten EA, Dutta Aloke K. Three-dimensional quantitative structure-activity relationship (3D QSAR) and pharmacophore elucidation of tetrahydropyran derivatives as serotonin and norepinephrine transporter inhibitors. J Comput Aided Mol Des. 2008; 22(1):1–17. [PubMed: 18060532]
29. Boehm, H-J.; Schneider, G., editors. Virtual Screening for Bioactive Molecules. 2000. p. 307-308.
30. Rao B-C, Subramanian J, Sharma SD. Managing protein flexibility in docking and its applications. Drug Discovery Today. 2009; 14(7/8):394–400. [PubMed: 19185058]
31. Sali A, Blundell TL. Comparative protein modelling by satisfaction of spatial restraints. J Mol Biol. 1993; 234(3):779–815. [PubMed: 8254673]
32. Chothia C, Lesk AM. The relation between the divergence of sequence and structure in proteins. Embo J. 1986; 5(4):823–826. [PubMed: 3709526]
33. Indarte M, Madura JD, Surratt CK. Dopamine transporter comparative molecular modeling and binding site prediction using the LeuTAa leucine transporter as a template. Proteins Struct, Funct, Bioinf. 2008; 70(3):1033–1046.
34. Aronson NN, Halloran BA, Alexyev MF, Amable L, Madura JD, Pasupulati L, Worth C, Van Roey P. Family 18 chitinase-oligosaccharide substrate interaction: subsite preference and anomer selectivity of Serratia marcescens chitinase A. Biochem J. 2003; 376(Pt 1):87–95. [PubMed: 12932195]
35. Oshiro C, Bradley EK, Eksterowicz J, Evensen E, Lamb ML, Lanctot JK, Putta S, Stanton R, Grootenhuis PDJ. Performance of 3D-Database Molecular Docking Studies into Homology Models. J Med Chem. 2004; 47(3):764–767. [PubMed: 14736258]
36. Kairys V, Fernandes MX, Gilson MK. Screening Drug-Like Compounds by Docking to Homology Models: A Systematic Study. J Chem Inf Model. 2006; 46(1):365–379. [PubMed: 16426071]
37. Martin YC. 3D database searching in drug design. J Med Chem. 1992; 35(12):2145–2154. [PubMed: 1613742]

38. Martin YC, Bures MG, Danaher EA, DeLazzer J, Lico I, Pavlik PA. A fast new approach to pharmacophore mapping and its application to dopaminergic and benzodiazepine agonists. J Comput-Aided Mol Des. 1993; 7(1):83–102. [PubMed: 8097240]
39. Wang S, Zaharevitz DW, Sharma R, Marquez VE, Lewin NE, Du L, Blumberg PM, Milne GWA. The Discovery of Novel, Structurally Diverse Protein Kinase C Agonists through Computer 3D-Database Pharmacophore Search. Molecular Modeling Studies. J Med Chem. 1994; 37(26):4479–4489. [PubMed: 7799398]
40. Kaminski JJ, Rane DF, Snow ME, Weber L, Rothofsky ML, Anderson SD, Lin SL. Identification of Novel Farnesyl Protein Transferase Inhibitors Using Three-Dimensional Database Searching Methods. J Med Chem. 1997; 40(25):4103–4112. [PubMed: 9406600]
41. Nicklaus MC, Neamati N, Hong H, Mazumder A, Sunder S, Chen J, Milne GWA, Pommier Y. HIV-1 Integrase Pharmacophore: Discovery of Inhibitors through Three-Dimensional Database Searching. J Med Chem. 1997; 40(6):920–929. [PubMed: 9083480]
42. Wang S, Sakamuri S, Enyedy IJ, Kozikowski AP, Deschaux O, Bandyopadhyay BC, Tella SR, Zaman WA, Johnson KM. Discovery of a novel dopamine transporter inhibitor, 4-Hydroxy-1-methyl-4-(4-methylphenyl)-3-piperidyl 4-methylphenyl ketone, as a potential cocaine antagonist through 3D-database pharmacophore searching. Molecular modeling, structure-activity relationships, and behavioral pharmacological studies. J Med Chem. 2000; 43(3):351–360. [PubMed: 10669562]
43. Indarte M, Liu Y, Madura JD, Surratt CK. Receptor-Based Discovery of a Plasmalemmal Monoamine Transporter Inhibitor via High-Throughput Docking and Pharmacophore Modeling. ACS Chem Neurosci. 2010; 1(3):223–233. [PubMed: 20352074]
44. Shoichet BK. Virtual screening of chemical libraries. Nature. 2004; 432(7019):862–865. [PubMed: 15602552]
45. Nolan TL, Lapinsky DJ, Talbot JN, Indarte M, Liu Y, Manepalli S, Geffert LM, Amos ME, Taylor PN, Madura JD, Surratt CK. Identification of a novel selective serotonin reuptake inhibitor by coupling monoamine transporter-based virtual screening and rational molecular hybridization. ACS Chem Neurosci. 201110.1021/cn200044x
46. Shen M-Y, Sali A. Statistical potential for assessment and prediction of protein structures. Protein Sci. 2006; 15(11):2507–2524. [PubMed: 17075131]
47. [accessed Sep 30, 2010] http://deposit.rcsb.org/validate
48. Andersen J, Taboureau O, Hansen KB, Olsen L, Egebjerg J, Stromgaard K, Kristensen AS. Location of the antidepressant binding site in the serotonin transporter: importance of Ser-438 in recognition of citalopram and tricyclic antidepressants. The Journal of biological chemistry. 2009; 284(15):10276–10284. [PubMed: 19213730]
49. Rupp A, Kovar KA, Beuerle G, Ruf C, Folkers G. A new pharmophoric model for 5-HT reuptake-inhibitors: differentiation of amphetamine analogues. Pharm Acta Helv. 1994; 68(4):235–244. [PubMed: 8208746]
50. Muszynski IC, Scapozza L, Kovar K-A, Folkers G. Quantitative Structure-Activity Relationships of Phenyltropanes as Inhibitors of Three Monoamine Transporters: Classical and CoMFA studies. Quant Struct-Act Relat. 1999; 18(4):342–253.
51. Irwin JJ, Shoichet BK. ZINC--a free database of commercially available compounds for virtual screening. J Chem Inf Model. 2005; 45(1):177–182. [PubMed: 15667143]
52. Wang W, Sonders MS, Ukairo OT, Scott H, Kloetzel MK, Surratt CK. Dissociation of High-Affinity Cocaine Analog Binding and Dopamine Uptake Inhibition at the Dopamine Transporter. Molecular Pharmacology. 2003; 64(2):430–439. [PubMed: 12869648]
53. Ukairo OT, Bondi CD, Newman AH, Kulkarni SS, Kozikowski AP, Pan S, Surratt CK. Recognition of Benztropine by the Dopamine Transporter (DAT) Differs from That of the Classical Dopamine Uptake Inhibitors Cocaine, Methylphenidate, and Mazindol as a Function of a DAT Transmembrane 1 Aspartic Acid Residue. Journal of Pharmacology and Experimental Therapeutics. 2005; 314(2):575–583. [PubMed: 15879005]
54. Anand K, Ziebuhr J, Wadhwani P, Mesters JR, Hilgenfeld R. Coronavirus Main Proteinase (3CLpro) Structure: Basis for Design of Anti-SARS Drugs. Science. 2003; 300(5626):1763–1767. [PubMed: 12746549]

55. Enyedy IJ, Lee S-L, Kuo AH, Dickson RB, Lin C-Y, Wang S. Structure-Based Approach for the Discovery of Bis-benzamidines as Novel Inhibitors of Matriptase. J Med Chem. 2001; 44(9): 1349–1355. [PubMed: 11311057]
56. Enyedy IJ, Ling Y, Nacro K, Tomita Y, Wu X, Cao Y, Guo R, Li B, Zhu X, Huang Y, Long Y-Q, Roller PP, Yang D, Wang S. Discovery of Small-Molecule Inhibitors of Bcl-2 through Structure-Based Computer Screening. J Med Chem. 2001; 44(25):4313–4324. [PubMed: 11728179]
57. Li R, Chen X, Gong B, Selzer PM, Li Z, Davidson E, Kurzban G, Miller RE, Nuzum EO, McKerrow JH, Fletterick RJ, Gillmor SA, Craik CS, Kuntz ID, Cohen FE, Kenyon GL. Structure-based design of parasitic protease inhibitors. Bioorganic & medicinal chemistry. 1996; 4(9):1421–1427. [PubMed: 8894100]
58. Que X, Brinen LS, Perkins P, Herdman S, Hirata K, Torian BE, Rubin H, McKerrow JH, Reed SL. Cysteine proteinases from distinct cellular compartments are recruited to phagocytic vesicles by Entamoeba histolytica. Molecular and biochemical parasitology. 2002; 119(1):23–32. [PubMed: 11755183]
59. Rajnarayanan RV, Dakshanamurthy S, Pattabiraman N. "Teaching old drugs to kill new bugs": structure-based discovery of anti-SARS drugs. Biochemical and biophysical research communications. 2004; 321(2):370–378. [PubMed: 15358186]
60. Selzer PM, Chen X, Chan VJ, Cheng M, Kenyon GL, Kuntz ID, Sakanari JA, Cohen FE, McKerrow JH. Leishmania major:Molecular Modeling of Cysteine Proteases and Prediction of New Nonpeptide Inhibitors. Experimental Parasitology. 1997; 87(3):212–221. [PubMed: 9371086]
61. Zuccotto F, Zvelebil M, Brun R, Chowdhury SF, Di Lucrezia R, Leal I, Maes L, Ruiz-Perez LM, Gonzalez Pacanowska D, Gilbert IH. Novel inhibitors of Trypanosoma cruzi dihydrofolate reductase. European Journal of Medicinal Chemistry. 2001; 36(5):395–405. [PubMed: 11451529]
62. Consortium TU. The universal protein resource (UniProt). Nucleic Acids Research. 2007; 35:D193–D197. [PubMed: 17142230]
63. Berman HM, Westbrook J, Feng Z, Gilliland G, Bhat TN, Weissig H, Shindyalov IN, Bourne PE. The Protein Data Bank. Nucleic Acids Research. 2000; 28(1):235–242. [PubMed: 10592235]
64. Discovery Studio Modeling Environment. Accelrys Software Inc; San Diego: 2010. p. 2.5.1
65. Sanchez R, Sali A. Large-scale protein structure modeling of the Saccharomyces cerevisiae genome. Proc Natl Acad Sci U S A. 1998; 95(23):13597–13602. [PubMed: 9811845]
66. Celik L, Sinning S, Severinsen K, Hansen CG, Moller MS, Bols M, Wiborg O, Schiott B. Binding of Serotonin to the Human Serotonin Transporter. Molecular Modeling and Experimental Validation. J Am Chem Soc. 2008; 130(12):3853–3865. [PubMed: 18314975]
67. Thijs Beuming LS, Javitch Jonathan A, Weinstein Harel. A Comprehensive Structure-Based Alignment of Prokaryotic and Eukaryotic Neurotransmitter/Na^+ Symporters (NSS) Aids in the Use of the LeuT Structure to Probe NSS Structure and Function. Mol Pharmacol. 2006; 70(5): 1630–1642. [PubMed: 16880288]
68. Molecular Operating Environment (MOE). Chemical Computing Group Inc., S. S. W; Suite #910, Montreal, QC, Canada, H3A 2R7:
69. Ponder Jay W, Case David A. Force fields for protein simulations. Adv Protein Chem. 2003; 66:27–85. [PubMed: 14631816]
70. Wang J, Cieplak P, Kollman PA. How well does a restrained electrostatic potential (RESP) model perform in calculating conformational energies of organic and biological molecules? J Comput Chem. 2000; 21(12):1049–1074.
71. Frank H. The Cambridge Structural Database: a quarter of a million crystal structures and rising. Acta Crystallogr. 2002; B58(3 No 1):380–388.
72. McMeeking B, Fletcher D. The United Kingdom Chemical Database Service: CDS. Cheminf Dev. 2004:37–67.
73. Halgren TA. Merck molecular force field. I. Basis, form, scope, parameterization, and performance of MMFF94. J Comput Chem. 1996; 17(5 & 6):490–519.
74. Halgren TA. Force fields: MMFF94. In: Encyclopedia of computational chemistry. Encyclopedia of computational chemistry. 1998; 2:1033–1035.
75. Maple. Forcefields: a general discussion. Encyclopedia of computational chemistry. 1998; 2:1015–1024.

76. Clark Alex M, Labute P. 2D depiction of protein-ligand complexes. J Chem Inf Model. 2007; 47(5):1933–1944. [PubMed: 17715911]

77. Lipinski CA, Lombardo F, Dominy BW, Feeney PJ. Experimental and computational approaches to estimate solubility and permeability in drug discovery and development settings. Adv Drug Deliv Rev. 2001; 46(1–3):3–26. [PubMed: 11259830]

78. Yung-Chi C, Prusoff WH. Relationship between the inhibition constant (KI) and the concentration of inhibitor which causes 50 per cent inhibition (I50) of an enzymatic reaction. Biochemical pharmacology. 1973; 22(23):3099–3108. [PubMed: 4202581]

79. Beitz E. TEXshade: shading and labeling of multiple sequence alignments using LATEX2 epsilon. Bioinformatics. 2000; 16(2):135–139. [PubMed: 10842735]

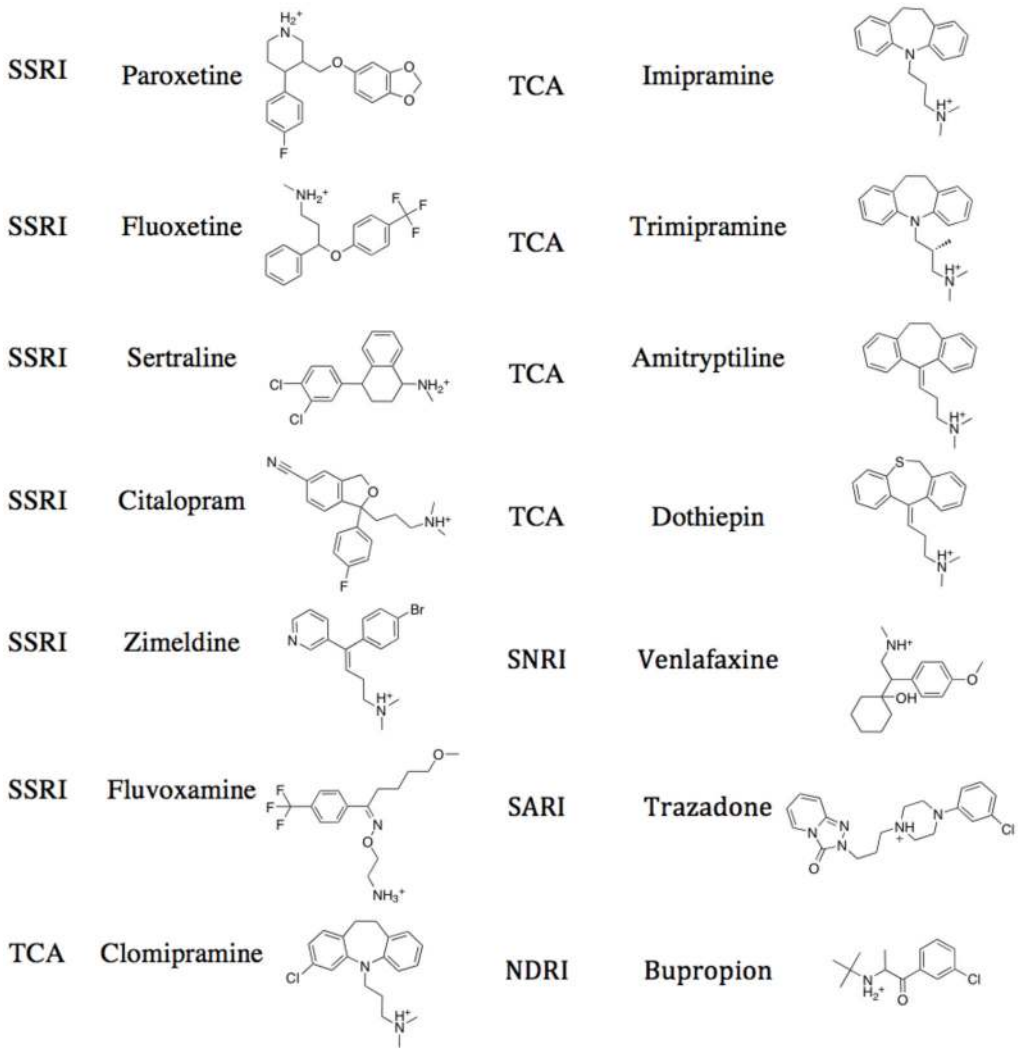

Figure 1.
Chemical structures of SERT inhibitors used to develop the pharmacophore.

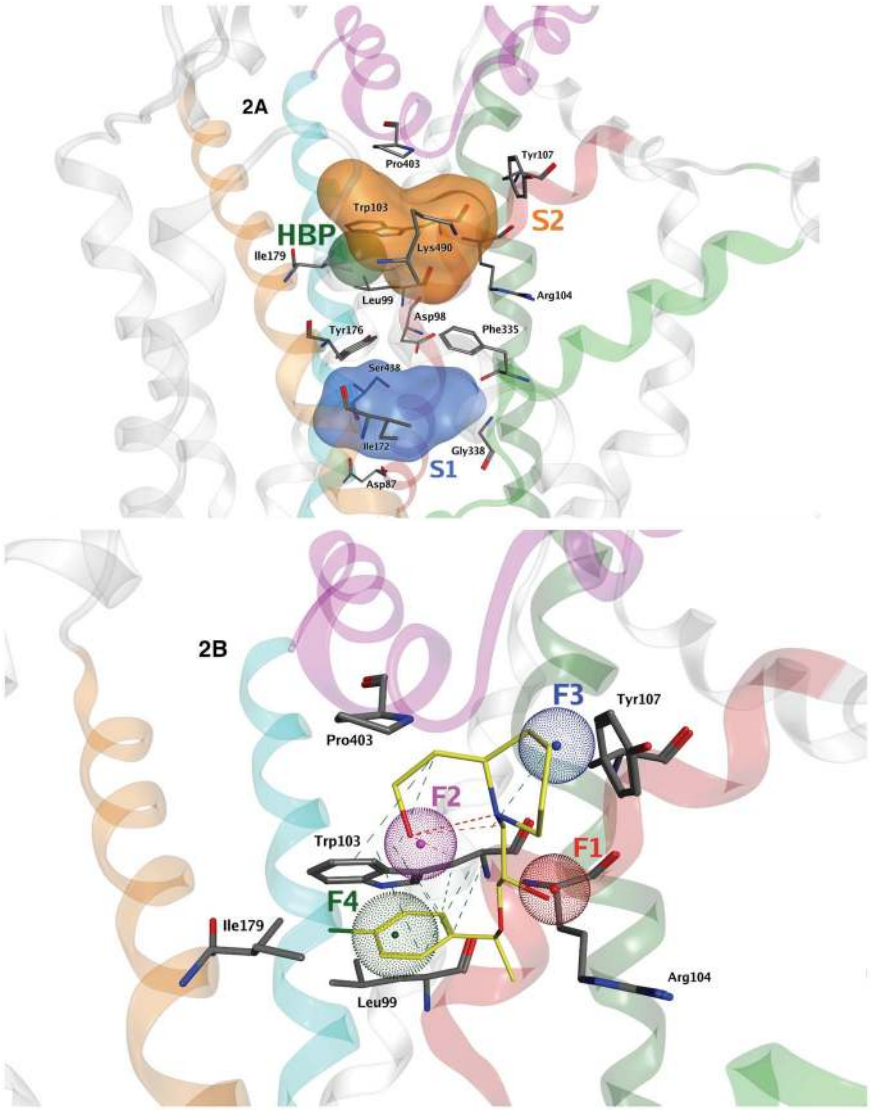

Figure 2.

Panel A: Ligand-accessible regions of SERT substrate and inhibitor binding pockets. Regions available to ligands in the S1 (blue), S2 (orange) and HBP (green) pockets are displayed as surfaces. The pocket employed for virtual screening combined the S2 and HBP. Residues defining each pocket are displayed as sticks (atomtype color). For clarity, the TM1 (red), TM3 (orange), TM6 (green), TM8 (cyan) and EL4 (pink) helices are highlighted. Panel B: The pharmacophore employed for VS was comprised of four features (dotted spheres). F1: Donor/acceptor (red). F2: Acceptor (pink). F3: Cation/acceptor (blue). F4: Hydrophobic/π ring (green). Predicted hydrophobic (green dashed lines) and H-bonding (red dashes lines) are shown for the VS hit compound SM-10 (yellow sticks with heteroatoms in green (halogen), red (oxygen) or blue (nitrogen).

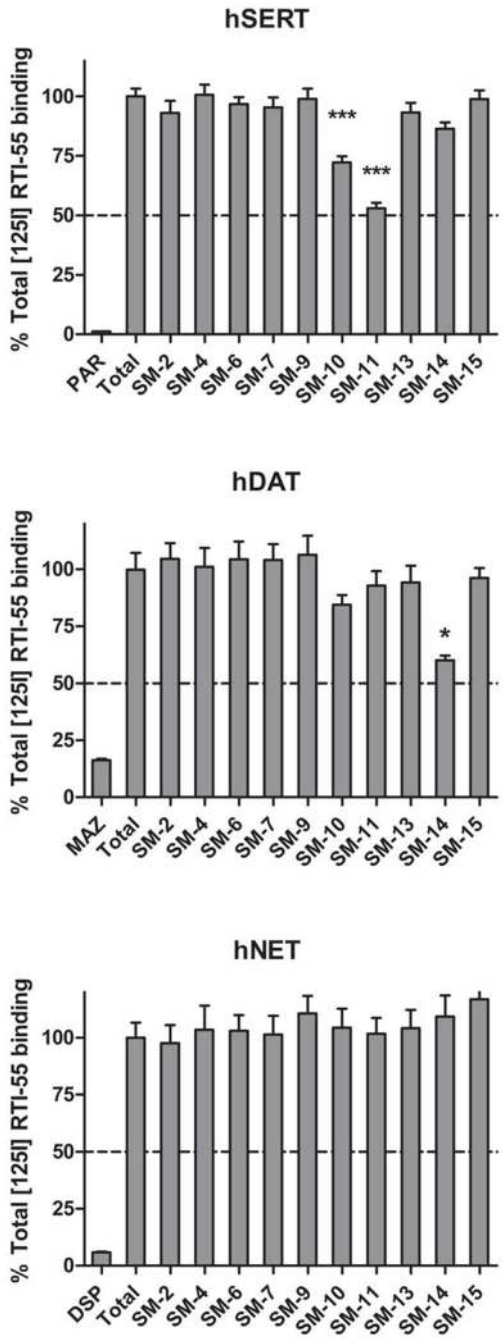

Figure 3.

VS hit compound in vitro MAT binding screen. Compounds at 10 μM final concentration were tested for the ability to inhibit [125I]-RTI-55 binding at hSERT HEK293 cells (top panel), hDAT N2A neuroblastoma cells (middle panel), or hNET HEK293 cells (bottom panel). Non-specific binding was assessed by the presence of 10 μM paroxetine (PAR), mazindol (MAZ) or desipramine (DSP) for SERT, DAT and NET, respectively. Data represent n=3 independent experiments performed in duplicate. Data are presented as the mean ± s.e.m. and were analyzed by one-way ANOVA with Dunnett's multiple comparison post-hoc test. *P < 0.05 vs. total binding for that assay. ***P < 0.0001 vs. total binding for that assay.

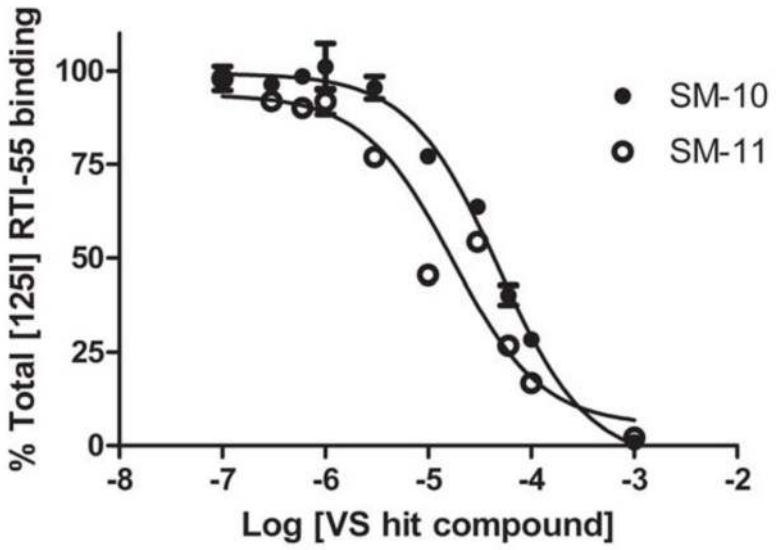

Figure 4.
Saturation binding of VS hit compounds SM-10 (closed circles) and SM-11 (open circles) at hSERT HEK293 cells. Binding affinity K_i values were determined via displacement of [^{125}I]-RTI-55. n=3 experiments.

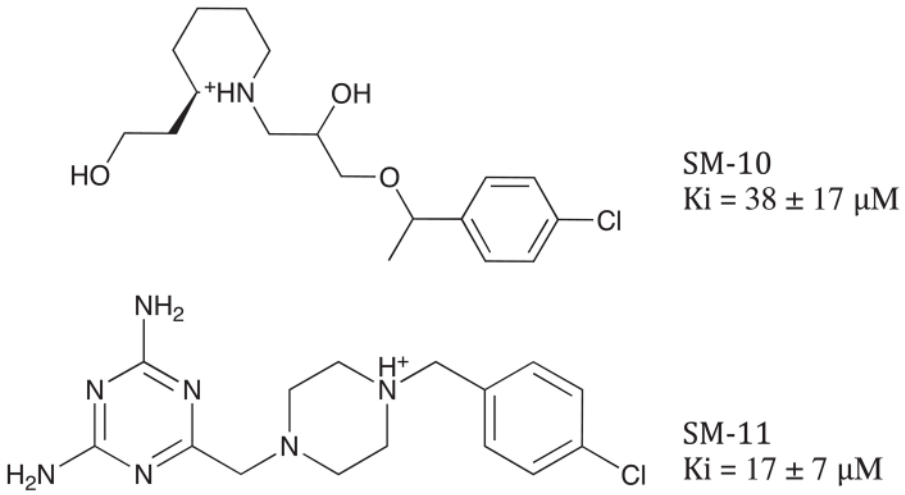

Figure 5.

VS hit compound in vitro serotonin uptake inhibition screen. Compounds at 10 μM final concentration were tested for the ability to inhibit [^{3}H]-serotonin uptake by hSERT HEK293 cells. Non-specific radioligand uptake was assessed by the presence of 10 μM paroxetine (PAR). Data represent n=3 independent experiments performed in duplicate. Data are presented as the mean ± s.e.m. and were analyzed by one-way ANOVA with Dunnett's multiple comparison post-hoc test. *P < 0.05 vs. total uptake for that assay. **P < 0.001 vs. total uptake for that assay.

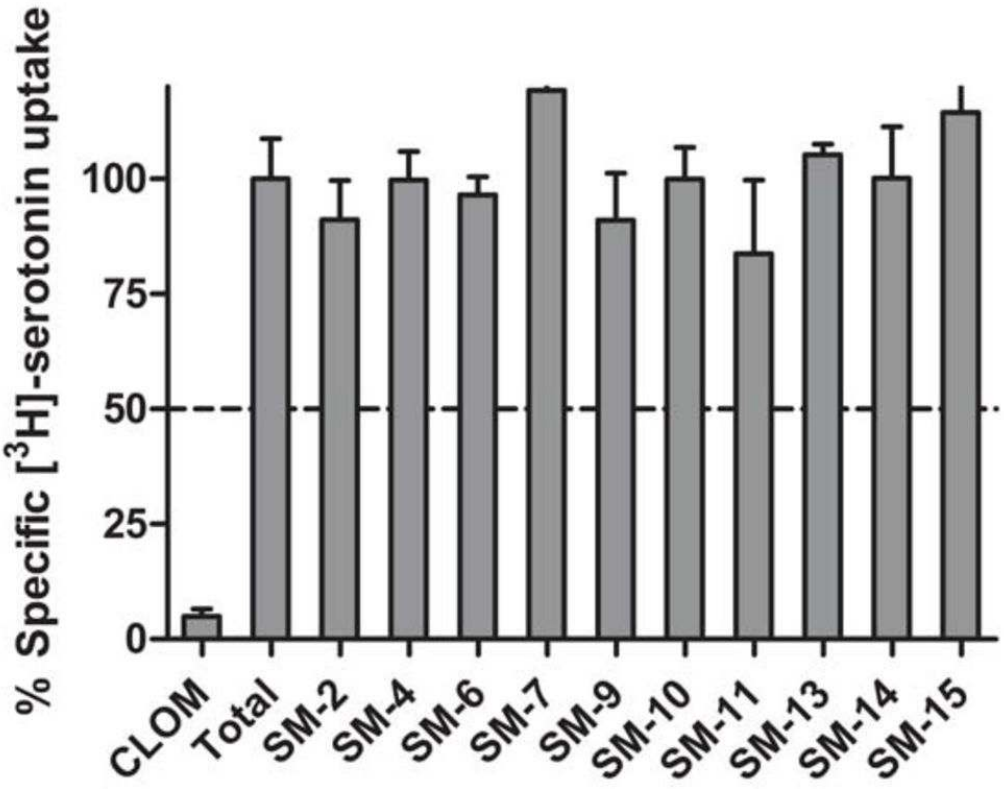

Figure 6.
Structures and hSERT binding affinities of SM-10 and SM-11.

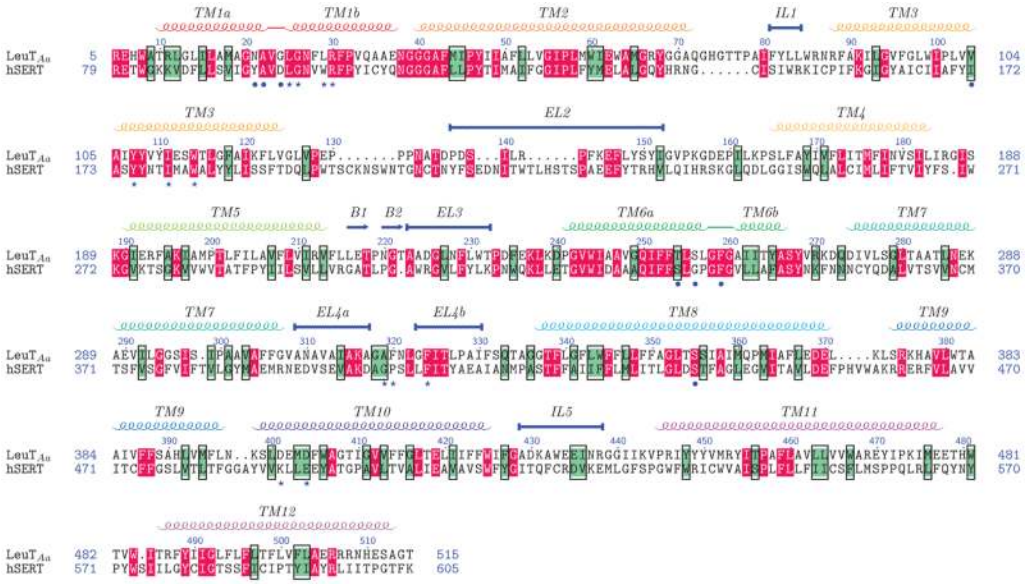

Figure 7.

Alignment of $LeuT_{Aa}$ and hSERT amino acid sequences used to build Model 1. Identical (blue) and similar (red) aligned residues are indicated. The dots and stars correspond to residues lining S1 and S2 pockets respectively. Transmembrane and connecting loop topology is displayed above the sequences. Gaps relative to the other sequence are represented by dots. Position of the residue in its respective chain is indicated before and after each line of sequence. The figure was prepared using TEXshade.[79]

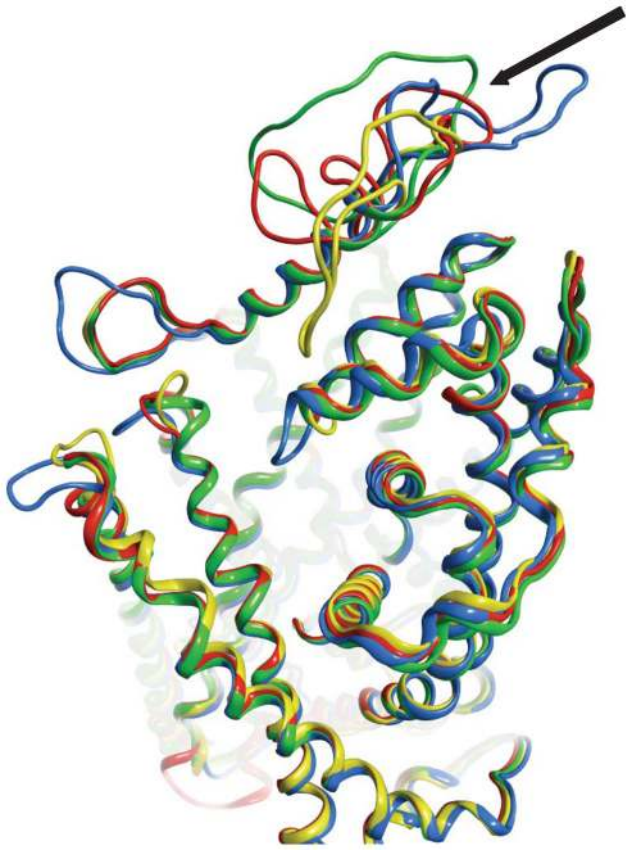

Figure 8.
Polypeptide backbone superposition of the four homology SERT models. Good overall spatial overlap was observed for Models 1 (Manepalli et al.; red), 2 (Beuming et al.;[67] blue), 3 (Yamashita et al.;[16] yellow) and 4 (Celik et al.;[66] green), with essentially perfect overlap of TM domains. EL2 (arrow) was the most divergent region among the four models.